N95-23831

# HYPERVELOCITY IMPACT SURVIVABILITY EXPERIMENTS FOR CARBONACEOUS IMPACTORS: PART II

T. E. Bunch
NASA Ames Research Center
Moffett Field, CA 94035-1000

Julie M. Paque
SETI Institute
2035 Landings Drive
Mountain View, CA 94043

Luann Becker
Scripps Institute of Oceanography
University of California at San Diego, La Jolla, CA 92093

James F. Vedder
NASA Ames Research Center
Moffett Field, CA 94035-1000

Jozef Erlichman
TMA/Norcal
2030 Wright Ave., Richmond, CA 94804

## ABSTRACT

Hypervelocity impact experiments were performed to further test the survivability of carbonaceous impactors and to determine potential products that may have been synthesized during impact. Diamonds were launched by the Ames two-stage light gas gun into Al plate at velocities of 2.75 and 3.1 km $sec^{-1}$. FESEM imagery confirms that diamond fragments survived in both experiments. Earlier experiments found that diamonds were destroyed on impact above 4.3 km $sec^{-1}$. Thus, the upper stability limit for diamond on impact into Al, as determined from our experimental conditions, is between 3.1 and 4.3 km $sec^{-1}$.

Particles of the carbonaceous chondrite Nogoya were also launched into Al at a velocity of 6.2 km $sec^{-1}$. Laser desorption ($L^2MS$) analyses of the impactor residues indicate that the lowest and highest mass polycyclic aromatic hydrocarbons (PAHs) were largely destroyed on impact; those of intermediate mass (202-220 amu) remained at the same level or increased in abundance. In addition, alkyl-substituted homologs of the most abundant pre-impacted PAHs were synthesized during impact. These results suggest that an unknown fraction of some organic compounds can survive low to moderate impact velocities and that synthesized products can be expected to form up to velocities of, at least, 6.5 km $sec^{-1}$.

We also present examples of craters formed by a unique microparticle accelerator that could launch micron-sized particles of almost any coherent material at velocities up to ~15 km $sec^{-1}$. Many of the experiments have a direct bearing on the interpretation of LDEF craters.

## INTRODUCTION

The experimental results presented here are part of a continuing program aimed at determining characteristics of carbonaceous matter that has sustained hypervelocity impact. The initial results and objectives were presented at the Second LDEF Post-Retrieval Symposium (ref. 1).

Observations of LDEF impact craters indicate that a small but unknown fraction of the craters contain dark residues, possibly carbon-bearing (e. g., refs. 2 and 3). Information on the behavior of carbonaceous materials on impact is sparse (e. g., ref. 4), although Peterson *et al.*, (1991) (ref. 5) performed shock experiments on amino acid survivability. Two of the three crystalline forms of carbon, diamond and graphite are known to occur in meteorites (ref. 6) and diamond occurs in the interstellar medium (ISM) (ref. 7). Amorphous carbon and poorly crystallized graphite (PCG) in carbonaceous chondrites form the bulk of their carbon inventories together with many organic compounds including polycyclic aromatic hydrocarbons (PAHs) that are also found in the ISM (ref. 8). These and other organic compounds may occur in comets (e. g., ref. 9). The possibility exists that LDEF sampled carbonaceous-bearing particles from all of these environments. The information contained within carbonaceous impactors is vital to understanding their origin and significance.

In attempting to characterize and interpret LDEF carbonaceous residues, several first-order questions are being addressed: 1) Can carbon crystalline phases and organic compounds survive low velocity ($\leq 7$ km sec$^{-1}$) impact, and if they do survive, what are their characteristics? 2) If they do not survive impact, what are their breakdown products or shock synthesized products, if any? Light gas gun hypervelocity experiments have been conducted to constrain, within our experimental capabilities, these and other issues. Experiments to further refine techniques and establish additional impactor (projectile) criteria are continuing.

Preliminary results of morphological, compositional, and structural studies made on carbonaceous-bearing experimentally-formed impact residues are given in this report. In addition, some interesting results of experimental impacts via a unique microparticle accelerator (MPA) that were performed between 1970 and 1973 are presented. The data and samples were archived after the MPA was shut down nearly 18 years ago and were just recently reexamined. Only a portion of the MPA experiments were published; and those results, together with new data, are useful in the interpretation of LDEF craters and their residues.

## LIGHT GAS GUN EXPERIMENTS: SAMPLE SELECTION, EXPERIMENTAL AND ANALYTICAL TECHNIQUES

### Sample Selection and Experimental Conditions

An earlier study (ref. 1), indicated that diamond appears to be totally destroyed on impact into Al at speeds $> 4.3$ km sec$^{-1}$. Experiments at lower velocities (2.75 and 3.1) have been performed in order to determine the velocity at which the diamond structure is at least partially retained on impact. An additional higher velocity experiment (5.5 km sec$^{-1}$) was made to enhance the diamond impactor melt characteristics. The earlier study also indicated that most of the higher mass PAHs (polycyclic aromatic hydrocarbons) in the Murchison meteorite survived impact at 5.9 km sec$^{-1}$ and there was some evidence that some PAHs had been synthesized. In order to confirm these findings and explore them further, we launched particles of the Nogoya meteorite, which has twice the total amount of carbon, into an Al target (6061 alloy) at 6.2 km sec$^{-1}$. For experiments of this type, the Ames light gas gun (LGG) is limited to acceleration velocities of $< 6.5$ km sec$^{-1}$. Peak pressures and temperatures cannot be directly measured.

## Experimental Methodology

Two-stage Light Gas Gun Experiments

Projectile grains were loaded into a small (3 mm cavity) Al carrier cup, capped with an Al plate and fitted into a sabot for launching. The two-stage light gas gun (Figure 1) accelerates the sabot down a rifled barrel (1.2 m long; bore dia. = 9 mm) to velocities of ≈ 2-6.5 km $sec^{-1}$ depending on the amount of the powder charge (first stage), which in turn determines the speed of the deformable ram that compresses hydrogen gas (second stage). When the gas reaches a certain critical pressure, a diaphragm ruptures and the gas propels the sabot down the barrel. At the end of the barrel, the sabot, carrier, and particles are separated in a "blast" chamber, particle velocities are electronically recorded, the in-flight particles are photographed, and the particles continue on to impact with the target plate (at 90° to the target) in an evacuated chamber (vacuum pressures nominally <1 mm of Hg). The impacted plate also serves as a witness plate with a 2.5 cm dia. hole through which the carrier travels. This technique allows only particles to impact, the alignment of the launch can be measured, and the range in diameters of the launched particles at the impact point can be measured from the holes in the mylar covering which is attached beneath the hole. This cluster shot approach is necessary for projectiles < 1.0 mm in diameter as smaller grains cannot be individually launched.

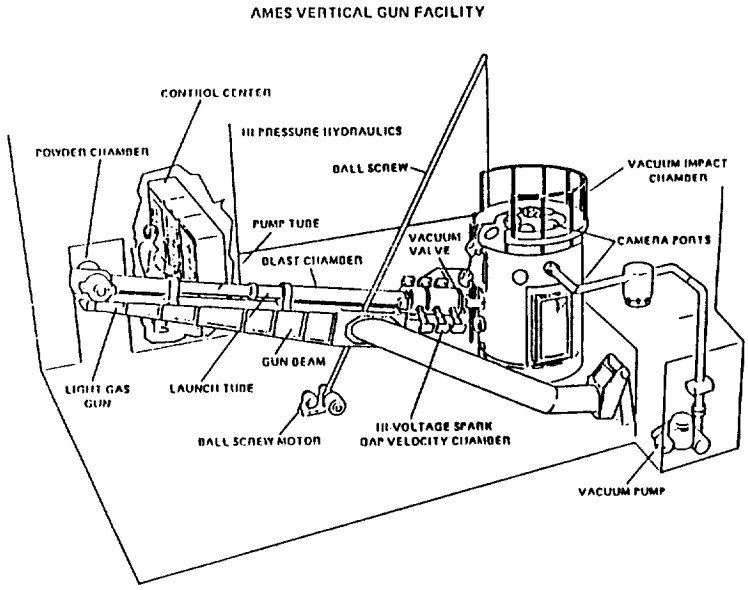


Figure 1

## Observational and Analytical Techniques

Samples were dry cut from the target plate. Craters and retained impactor debris were first observed by an optical light microscope, then by field emission scanning electron microscopy (FESEM). Samples were then analyzed for impactor residue by light element equipped energy dispersive spectroscopy (EDS).

Major Analytical Technique

*Laser Ionization Mass Spectrometry ($L^2MS$).* The two-step laser methodology has been described elsewhere (ref. 10). In the first step, the pulsed output of a $CO_2$ laser (10.6 μm; 20 mJ/pulse; 10 μsec pulse width; 5-Hz repetition rate) is focused onto a small stainless steel disk (~1 mm diameter) containing the meteorite sample. The infrared (IR) radiation is readily absorbed by the meteorite minerals and causes the ejection of intact neutral molecules from their surfaces in a rapid, laser-induced thermal desorption process. The fact that desorption dominates over decomposition in rapid laser heating processes is well documented (refs. 10, 11). The sample can be rotated manually in order to expose fresh surface to the desorption laser. After an appropriate time delay (~130 μsec), the fourth harmonic of a Nd:YAG laser (266 nm; 1.5-2.0 mJ/pulse; 10-nsec pulse width; 5-Hz repetition rate) is used to induce 1+1 resonance-enhanced multiphoton ionization (REMPI) of the desorbed

molecules in an interaction region about 5 mm from the surface. REMPI causes soft ionization so that the parent ions of the desorbed aromatic compounds almost exclusively dominate the spectrum. Total ionization efficiency is about a factor of 100 to 1000 greater than that of methods where ions are directly produced on a surface. One of the advantages to the $L^2MS$ system is the spatial and temporal separation of the desorption and ionization which results in more control than in one-step desorption /ionization processes. The laser-generated ions are mass separated in a linear TOF system (mass resolution = 500) and detected with a microchannel plate array. Data for the meteorite samples were averaged over 100 laser shots, although a complete mass spectrum can be obtained from a single shot.

Samples were prepared using MALDI (matrix assisted laser desorption ionization). Previous reports have shown that laser desorption of neutral molecules can be improved by spraying a fine layer of sample on top of a matrix that absorbs at the wavelength of the laser (ref. 12). For our $L^2MS$ system, the organic substrate sinapinic acid was used as the matrix. The matrix is sprayed directly onto the stainless steel disc (100 ng/mm$^2$) insuring that the substrate is evenly dispersed over the entire surface of the disc. The impacted meteorite sample (sonicated in toluene) is then sprayed on top of the sinapinic acid film. The sample disc is mounted on a 7-mm diameter teflon probe tip and is introduced to the TOF mass spectrometer through a separate antechamber pumped down to zero millitorr before introducing it to the high vacuum ($10^{-7}$ torr) of the system. Sample introduction takes about two minutes and the spectrum can be recorded immediately thereafter.

## RESULTS

*Diamond Craters.* Craters formed by launching diamond into Al at 2.75 and 3.1 km sec$^{-1}$ (Figs. 2-3) show morphological features similar to those formed at higher velocities (4 - 6.1 km sec$^{-1}$; Fig. 4). The crater morphologies resemble penetration funnels more than they do classical craters formed by other impactors. The depth to diameter ratio is 1-1.6 for craters formed < 4 km sec$^{-1}$ and exceeds 1.5 for craters formed at ≈ 6 km sec$^{-1}$.

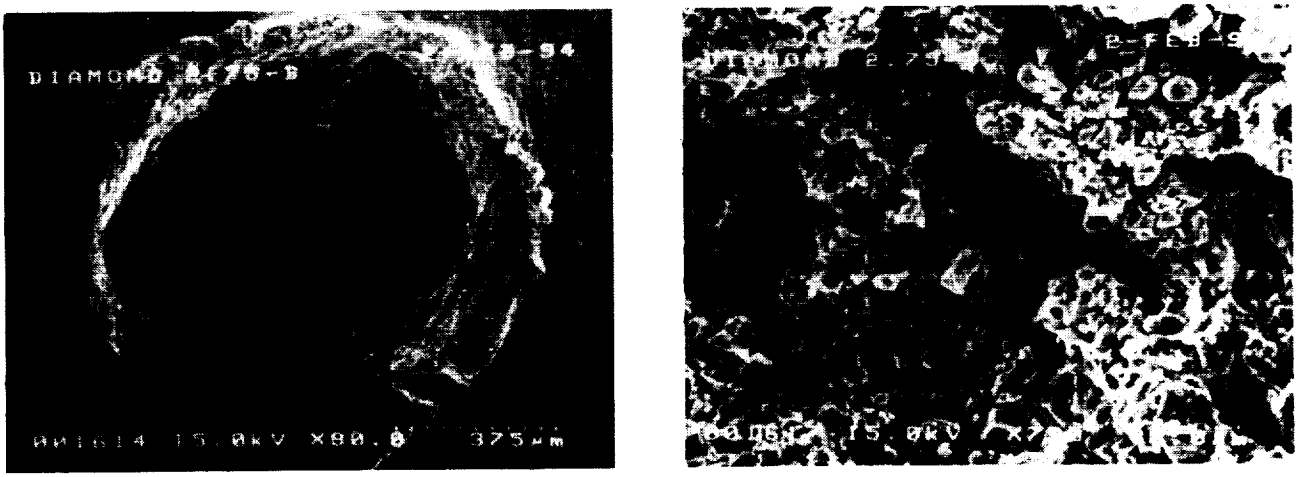

Fig. 2. FESEM images. (a) Diamond impact crater made at 2.75 km sec$^{-1}$. Note the ridge in the center and twin holes on either side. Apparently, the projectile broke into two main pieces soon after contact with the target. Arrow indicates ridge and area of 2b. (b) Enlargement near arrow showing micron to submicron fragments of intact diamond.

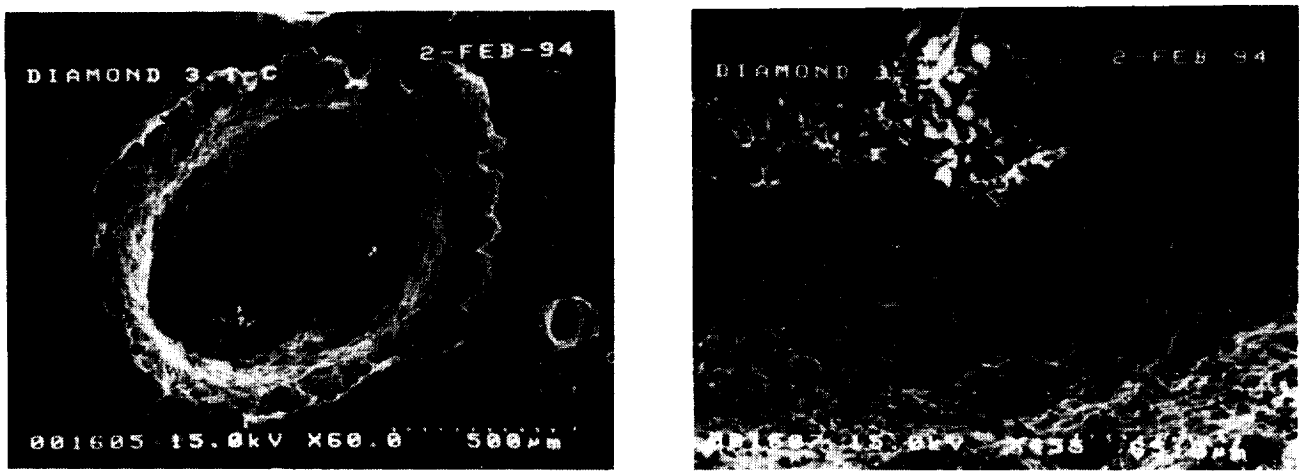


Fig. 3. (a) Diamond impact crater made at 3.1 km $sec^{-1}$. Arrow points to a ledge half way into the crater and the fragmented diamond in b. (b) Clump of fragmented, intact diamond.

Figure 3 shows a typical diamond crater formed at 3.1 km $sec^{-1}$. Raman spectroscopy of this crater indicates a strong band at 1330 $cm^{-1}$ (diamond) and less intense bands at 1360 and 1620 $cm^{-1}$ (PCG). In addition, a cluster of fragmented diamond can be seen on a ledge of the crater in Fig. 3a. Another launch at lower velocity (2.75 km $sec^{-1}$) shows abundant fragments in the center of the crater (Fig. 2). In our earlier report (ref. 1), we found evidence that some of the diamond may have actually melted (at 5 km $sec^{-1}$), although the carbon spherules observed in those craters may have been only carbon coated Al-melt spherules. To further investigate the problem, we launched diamond (0.3 - 0.5 mm dia.) into Al plate at 5.98 km $sec^{-1}$. FESEM examination of one crater (Fig. 5) illustrates the extreme P-T conditions that exist in shock impact. The open arrow points to a small, euhedral diamond fragment (0.012 mm in dia.) resting on a melt puddle of mostly carbon with a small amount of Al (solid arrows). The fragment may be ejecta from a nearby crater. Shrinkage cracks are very evident in the melt puddles and strongly infer derivation from a rapidly cooled melt.

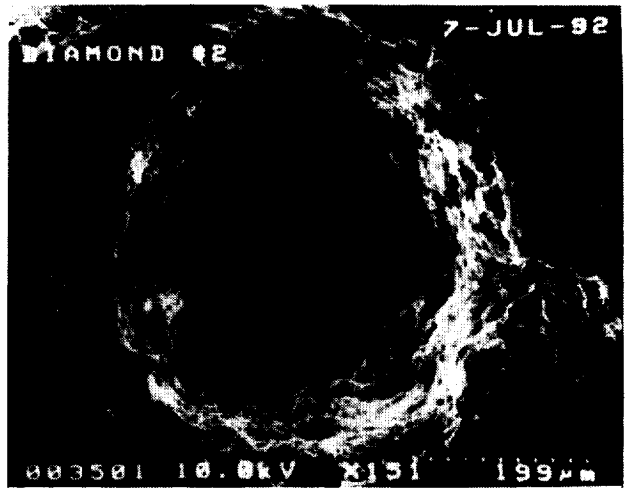


Fig. 4. Diamond crater made at 5.1 km $sec^{-1}$. Note the great depth and irregular cavity. Essentially no residual diamond; only PGC.

*Nogoya Meteorite Impactor Residues.* The PAH compositions of Nogoya have never been determined and we report here for the first time the PAH species from mass 128 to 300 (amu). The prelaunch PAH composition from $L^2MS$ analyses is shown in Fig. 6a and Table 1 below.

Table 1. PAHs in prelaunched Nogoya.

| Mass (amu) | Compound | B.P. (°C) (refs. 13, 14) |
|---|---|---|
| 178 | phenanthrene/anthracene* | 340 |
| 192 | methyl-phenanthrenes/anthracenes* | 278,196 |
| 202 | pyrene/fluoranthene* | 393, 375 |
| 206 | $C_{16}$-alkylphenanthrenes/anthracenes* | NA |
| 220 | $C_{17}$-alkylphenanthrenes/anthracenes* | NA |
| 252 | perylene | 350-400 |
| 276 | benzoperylene | 415 |
| 300 | coronene | 525 |

* These are possible assignments of the observed peaks; different isomers of PAHs cannot be distinguished by $L^2MS$. NA = not available.

Nogoya differs from Murchison in its PAH content by not having naphthalene (mass 128) or any of the alkyl-substituted species (homologs) of naphthalene (mass 142, 154, 170, 198), *e. g.*, 2-methyl naphthalene (mass 142). *Note*: a single alkyl substitution is a univalent aliphatic radical attached to the PAH structure; $CnH_2n+1$ = 14 or $CH_2$. Alkylation comes from the "cracking of the polymer" or the loss of $CH_2$ from a polymer (ref. 15) that is concentrated in constituent kerogens of the meteorite and attaches itself to the PAH benzene ring structure during a thermal event. Generally speaking, the greater the alkylation of PAHs, the lower the formation temperature (ref. 16). For example, PAHs formed at 2000°C have no alkyl substitutions; 400°C, a few and at 150°C, up to 6 alkyl carbons (ref. 17).

We launched granules of Nogoya matrix (0.1-0.2 mm dia.) into Al plate at 6.2 km $sec^{-1}$. The post-impact PAH contents are given in Fig. 6b and compared with the prelaunched samples in Table 2.

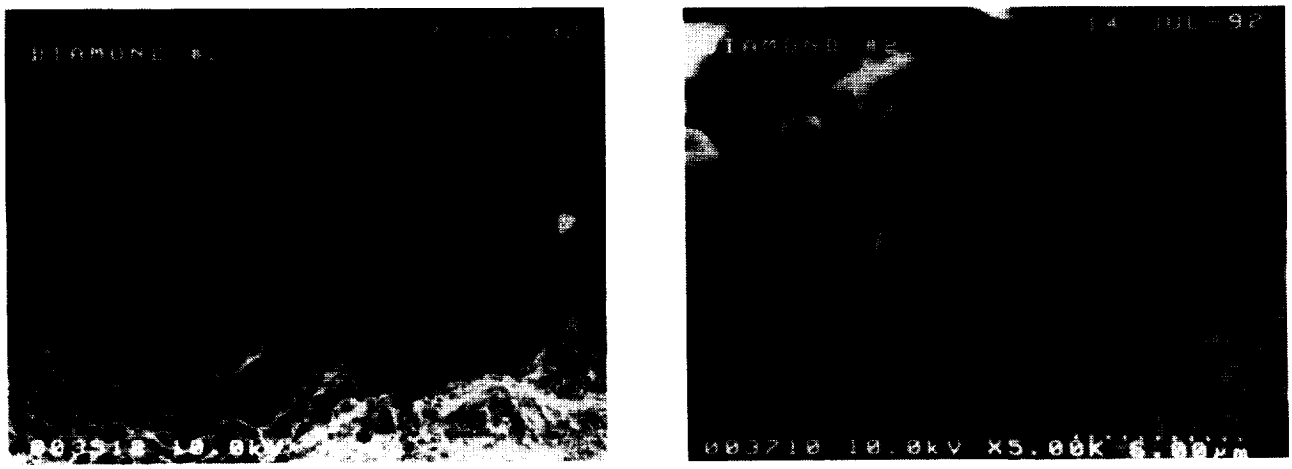

Fig. 5. (a) Diamond crater (enlarged area from Fig. 4) showing a diamond fragment (ejecta?) and two diamond melt "puddles" on the upper wall of the crater. (b) Enlargement of "puddle". Note shrinkage cracks.

## MICROPARTICLE ACCELERATOR EXPERIMENTS

### Instrument Description and Experimental Conditions

A unique microparticle accelerator (MPA), which produced high velocity, micron-sized projectiles of any cohesive material, was developed in the early years of the space age (ref. 18) and operated for 4 years until it was, unfortunately, shut-down. The samples and data were archived and forgotten for 18 years. We show a few examples of those experiments and discuss aspects of the accelerator because many of the experiments have a direct bearing on the interpretation of craters on LDEF. We plan to inventory the experimental results and samples and make the information available to interested investigators.

Although this accelerator is in the electrostatic class, its method of charging levitated particles surpassed in many ways the commonly used method of contact charging used by other accelerators. Single particles were charged by ion bombardment in an electrodynamic levitator. The vertical accelerator had four drift tubes, each initially at a high negative voltage. After injection of the projectile, each tube was grounded in turn at a time determined by the voltages and charge/mass ratio to give four acceleration stages with a total voltage equivalent to ≈ 1.7 MV. The delay times were set manually or controlled automatically by the particle's charge/mass ratio measured in the source by the operator just before ejection. At the entrance to the accelerator, the particle generated a signal that initiated the timing sequence. In the target chamber, detectors recorded the passage of the particle and provided information on charge, velocity, and position. Velocities between 0.5 and 15 km sec$^{-1}$ were routinely attained and 20 projectiles could be accelerated per day.

Table 2. PAH content in Nogoya after impact at 6.2 km sec$^{-1}$.

| Mass | Compound |
|---|---|
| **Missing:** | |
| 252 | perylene |
| 276 | benzoperylene |
| 300 | coronene |
| **Greatly reduced in content:** | |
| 178 | phenanthrene/anthracene |
| 192 | methyl-phenanthrenes/anthracenes |
| 202 | pyrene/fluoranthene |
| **About the same:** | |
| 206 | $C_{16}$-alkylphenanthrenes/anthracenes |
| **Increased:** | |
| 220 | $C_{17}$-alkylphenanthrenes/anthracenes |
| **Synthesized?** | |
| 234 | $C_{18}$-alkylphenanthrenes/anthracenes |

Table 3 lists some of the projectiles and targets that were used; many thousands of experiments were made over the lifetime of the accelerator. In all cases, the mass, velocity and size of the impactor, the depth to diameter ratio of the crater, and impact energy are known.

Scanning electron microscope images of a few cratering examples are shown in Figs. 7-9. We plan to start an analytical program to investigate impact residues of the impactors where feasible. Examples of residue signatures from ZnS crystals impacted into fused quartz at velocities of 4.6, 6.4 and 10.1 km sec$^{-1}$ are shown in Figs. 10 and 11. Although MPA craters are exceedingly small (<0.001-006 mm), they are similar in size to many of the craters on LDEF and the nominal size of craters examined on the COMET/SALIOUT Mission that mainly sampled particles from the Giacobini-Zinner Comet (J. Borg, pers. comm.). FESEM analyses of the ZnS craters indicate that Zn can still be detected on the rims of the MPA craters up to and including the 10.1 km sec$^{-1}$ crater (Fig. 11).

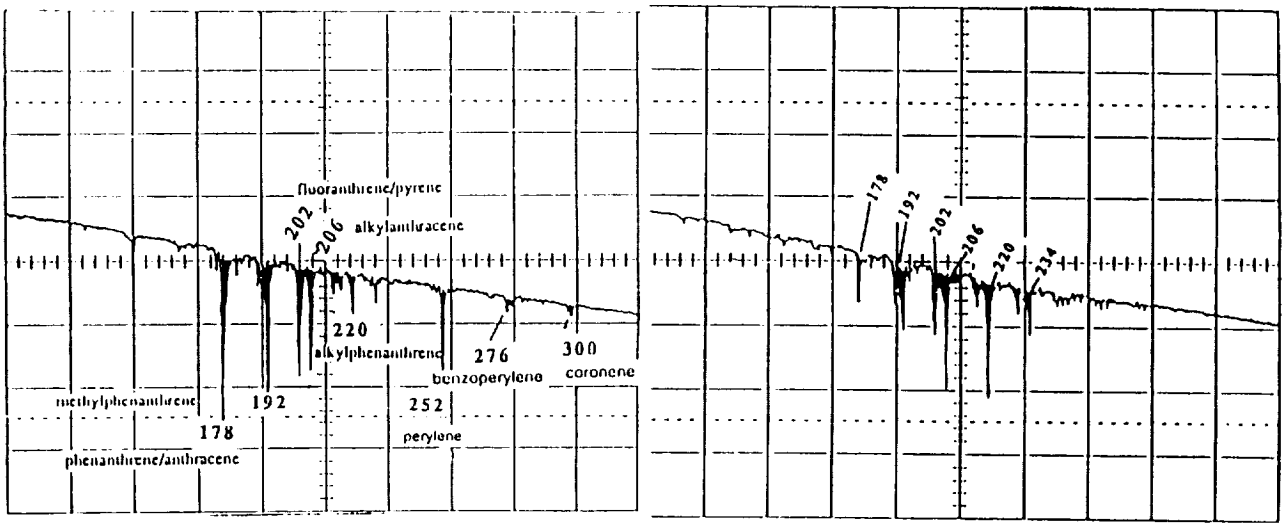


Fig. 6. (a) $L^2MS$ spectrum of non-impacted Nogoya. (b) After impact into Al at 6.2 km $sec^{-1}$.

Table 3. Examples of MPA projectiles and targets.

| Projectile | Velocity range (km $sec^{-1}$) | Targets |
|---|---|---|
| Polyethylene | 6-14 | glass |
| Polystyrene-DVB | 1-14 | glass, fused quartz, basalt glass, glass beads, lexan, Al, Cu stainless steel, feldspar silicates, diopside, olivine, chrysotile |
| Aluminum | 1.6-14 | Na glass, fused quartz, $Al_2O_3$, Al, Cu, olivine, feldspars, chrysotile. |
| Iron | 1-15+ | glass, basalt glass, fused quartz, olivine, diopside olivine, chrysotile. |
| $SiO_2$ | 1-13 | glass, lead glass, olivine, feldspar |
| Kaolin (clay) | 0.4-9.4 | glasses, feldspars, olivine, quartz, chrysotile |
| ZnS | 3.5-10.1 | fused quartz |
| Ti-glass | 2.4-13.7 | stainless steel, quartz, feldspar, Na glass and Pb glass |

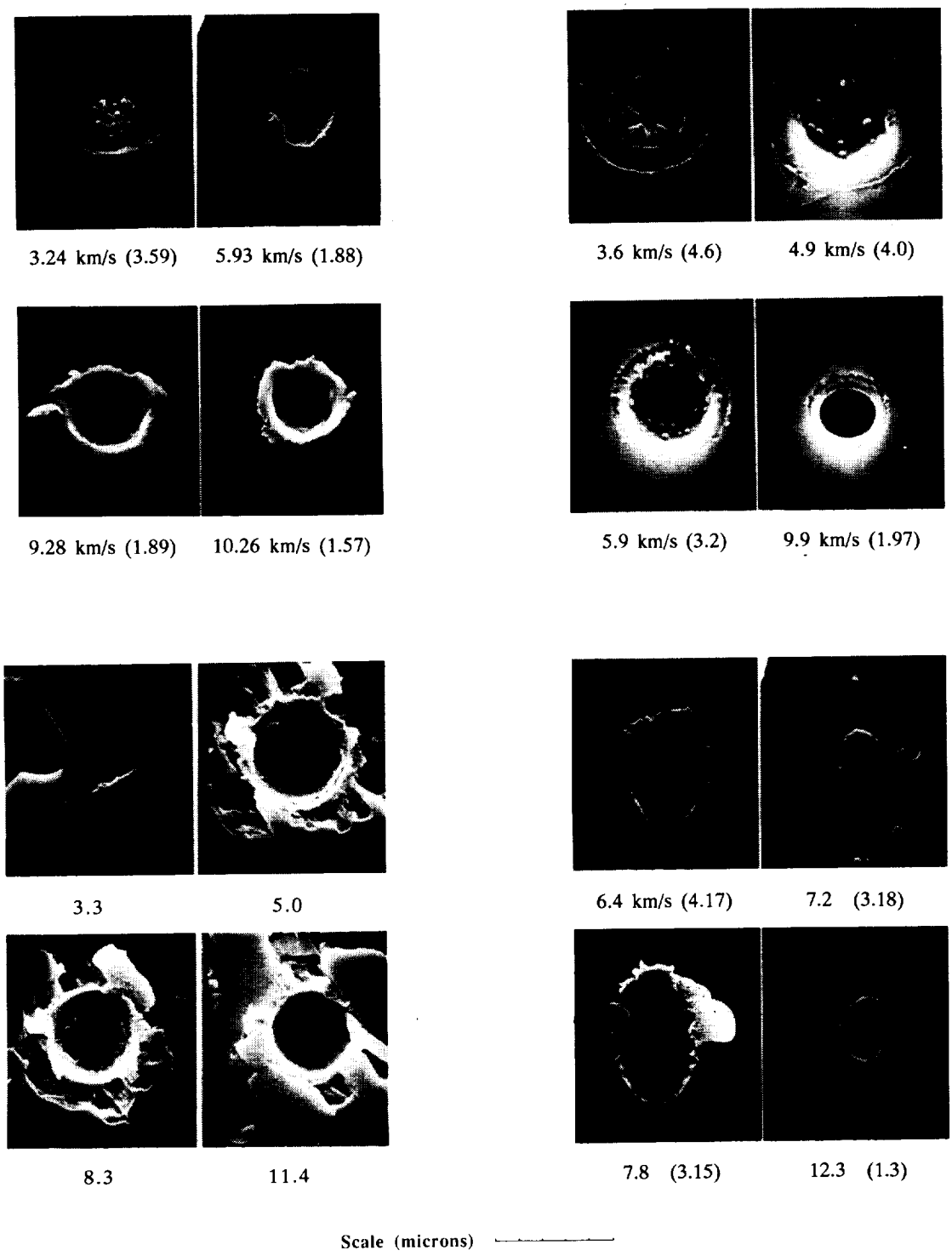


Fig. 7. SEM images of MPA craters: (a) Polystyrene launched into steel. (b) Polystyrene into fused quartz covered by a layer of Al + $MgF_2$. (c) Polystyrene into plagioclase. (d) Polystyrene into glass (60° from vertical). Impactor diameters in parentheses.

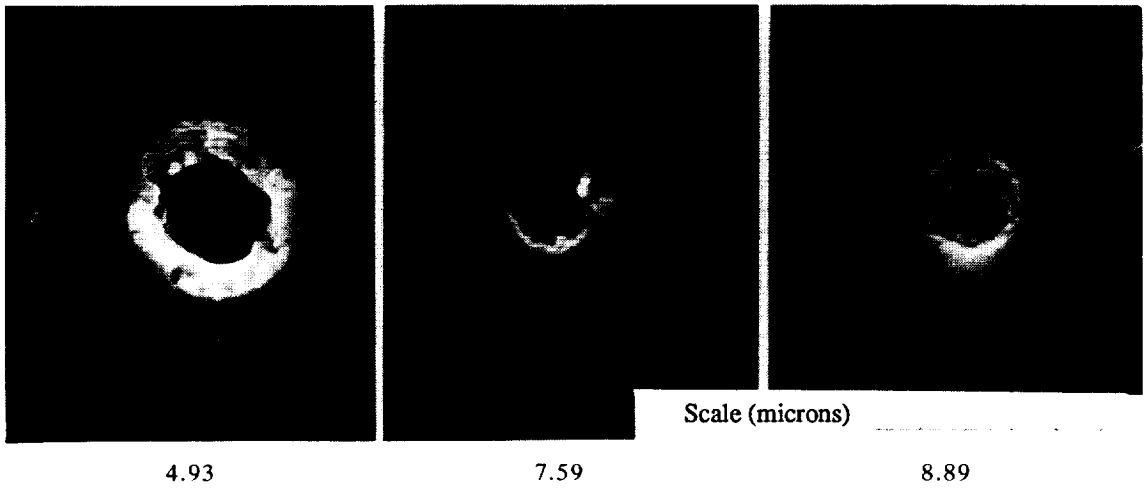


Fig. 8. Polystyrene into chrysotile (clay). Numbers refer to velocities (km $sec^{-1}$).

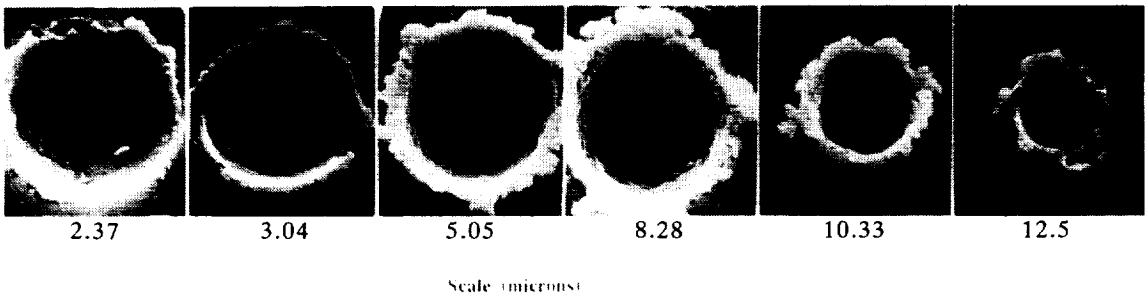


Fig. 9. Polystyrene into steel. Numbers refer to velocities (km $sec^{-1}$).

## DISCUSSION

*Diamond* From our impact experiments, we find that diamond can, at least, partially survive in impacts > 3.1 to < 4.3 km $sec^{-1}$. At 4.3 km $sec^{-1}$, diamond decomposes to PCG with some melting, and clear evidence for melting is developed at impact velocities of 5.5 km $sec^{-1}$. We can not directly measure peak pressures and temperatures of the experiments, although peak pressures can be extrapolated from equation-of-state information for Al and diamond and from the thermodynamic model that solves for peak stress generated by impactors and their targets (ref. 19). For diamond impacts of 2.75, 3.1, 4.3 and 5.5 km $sec^{-1}$, peak pressures are calculated as ≈ 35, 39, 60 and 84 GPa, respectively (M. Cintala. pers. comm.). The highest two pressures are sufficient to produce melting of anorthosite on impact into Al (ref. 20); diamond, which is 20% more dense than anorthosite should partially melt at these peak pressures. The time duration of peak pressures and temperatures for these impact events is probably on the order of $10^{-6}$ to $10^{-9}$ sec and the total crater formation time is probably less than a few μsec; extrapolated from data of (ref. 21). Although diamonds are not expected to be present as diamond IDPs from the interstellar medium, they are expected to be present as small grains (up to 10s of nanometers in dia.) in chondritic meterorites (ref. 22). The apparent low thermal stability of diamond under shock as shown in these experiments makes the study of any extracted intact meteoritic impact debris from LDEF craters impractical for diamond. On the other hand, our experiments establish a lower limit on diamond stability with respect to impacts into silicates during planetary accretion, *i. e.*, impacts into silicates > 3 km $sec^{-1}$, would probably destroy pertinent isotopic and noble gas information.

The irregular crater cavities may be attributed to the extreme ease with which diamond cleaves/fragments under impulsive loading. At the inception of impact in our experiments, diamond apparently broke into several large fragments and formed multiple-sized crater cavities at different depths within the crater, dependent on each fragment's mass. Clumps of finely fragmented intact diamonds for the 2.75 and 3.1 km $sec^{-1}$ experiments are observed in the bottom of each cavity of the crater (Figs. 2-3). This phenomenon is also observed to a lesser degree in craters formed by less coherent impactors, e. g., carbonaceous chondrite matrix projectiles which are composed of many weakly bound small grains. At higher impact velocities (ref. 1), the multiplicity of cavities per crater diminish, and the dominant morphology resembles a long, sinuous cavity with small branches from diamond fragmentation during the formation of the main crater cavity.

*Nogoya.* In our earlier report, we found that lower mass PAHs, naphthalene and alkyl-substituted naphthalenes (homologs), were absent in the impacted Murchison meteorite sample (5.9 km $sec^{-1}$). This absence was attributed to the higher volatility of these lower molecular weight PAHs which presumably volatilized during impact. In contrast, unshocked Nogoya does not contain PAHs below 178 amu and, in addition, contains PAHs above 252 amu (Fig. 6a). Figure 6b (shocked Nogoya) shows that the unsubstituted PAHs are either absent or greatly reduced by impact at 6.2 km $sec^{-1}$. This is expected for those below 202 amu, because of their higher volatility, but not for those above 252. For example, coronene has the highest boiling point


Fig. 10. SEM images of ZnS formed craters in glass: (a) 4.6 km $sec^{-1}$ crater. Impactor apparently separated into 3 fragments at impact. Impactor size was 0.0089 mm. (b) 6.4 km $sec^{-1}$ crater. Cracked surface is due to breakup of Au coating with time. Impactor dia. was 0.001 mm. (c) 10.1 km $sec^{-1}$ crater. Impactor dia. was 0.00066 mm. All crater outlines depart from circularity. All launches were 90° to the target and all rims contain detectable Zn.

of the common PAHs (Table 1) and is the most stable of aromatic compounds (ref. 23). The absence of coronene and benzoperylene in impacted Nogoya may be due to their low abundance in Nogoya, which is estimated from the $L^2MS$ spectrum (Fig. 6a) to be 1-5 ppm. The low concentration together with the known highly heterogeneous distributions of meteoritic organics may just be a sampling bias. However, this does not explain the absence of abundant perylene (252 amu) in shocked Nogoya. Moreover, as in the case for shocked Murchison, the alkylated homologs (206 and 220 amu) are the most abundant PAH species. In shocked samples of both meteorites, $C_{18}$-alkylphenanthrene/anthracene at amu 234 is present, probably as an impact-synthesized PAH. A detailed discussion with regard to the behavior of PAHs under shock loading conditions is beyond the scope of this report. We can conclude that, within our experimental and analytical constraints, some PAHs do survive impact at 6.2 km $sec^{-1}$, some are destroyed and a few appear to be synthesized (see Table 2).

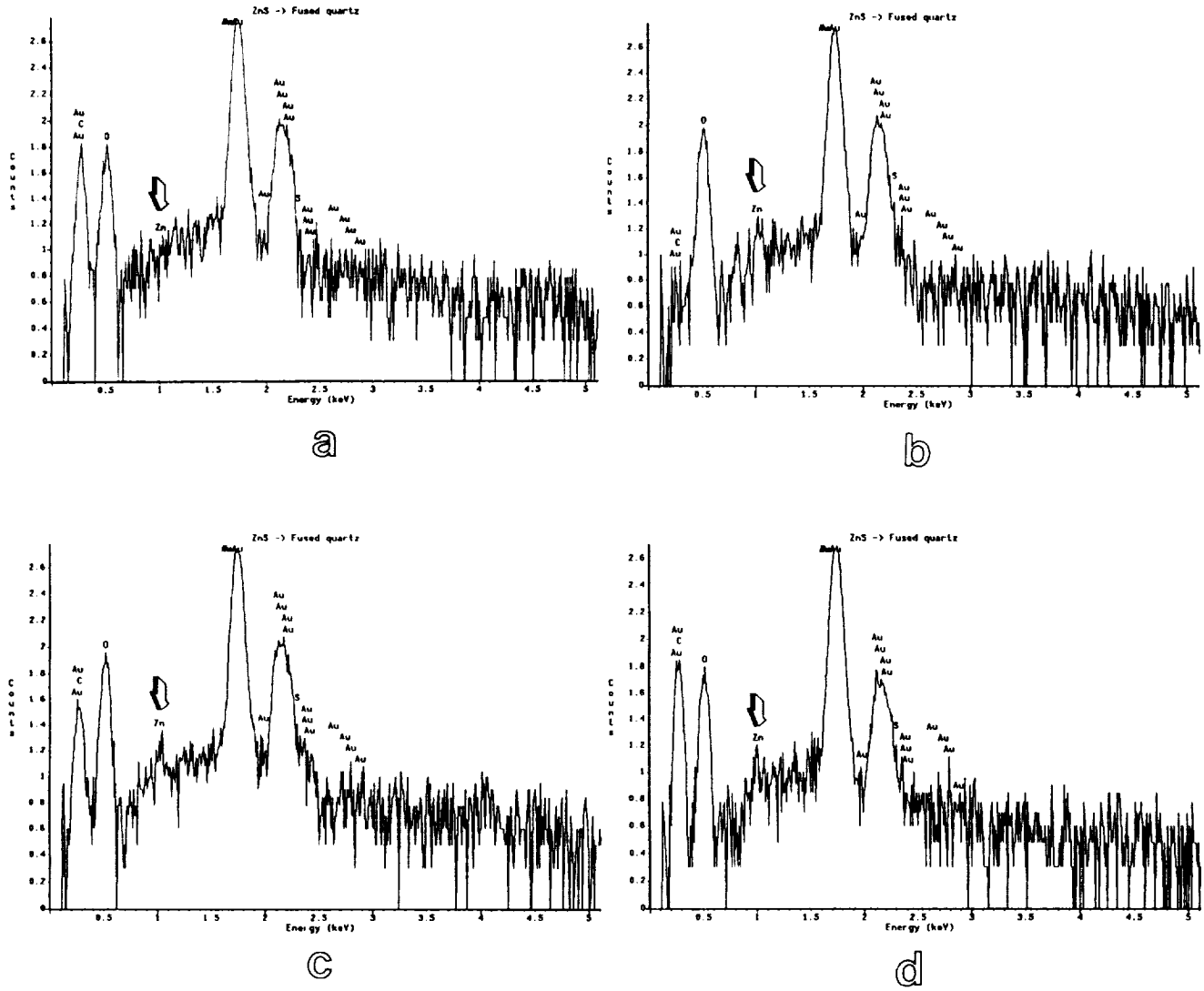


Fig. 11. SEM-EDS spectra of craters in Fig. 11 showing the presence of Zn residues. (a) Background. (b), (c), and (d) are the 4.6, 6.4 and 10.1 km $sec^{-1}$ craters, respectively.

## SUMMARY

A summary of the experimental results of the light gas gun experiments to date on carbonaceous impactors are given in Table 4.

Table 4. Summary of hypervelocity impact experiments involving carbonaceous impactors.

| Samples | Velocity (km $sec^{-1}$) | Remarks |
|---|---|---|
| Graphite | 3-5.95 | Graphite decomposed to various degrees of poorly characterized graphite (PCG). Correlation of highest disorder with distance away from crater bottom center. |
| Fullerenes | 4-6.2 | A small portion of fullerene impactors decomposed to disordered carbon. Fullerenes not formed from carbonaceous impactors. |
| Diamond | 2.75-5.95 | Diamond decomposed to PCG and vitreous/amorphous carbon above 4 km $sec^{-1}$ impact velocities. |
| Murchison | 4.35-5.98 | PAHs above molecular mass 178 mostly survived impact. Naphthalene and alkyl-substituted naphthalenes were destroyed. Additional alkyl homologs of phenanthrene-/anthracene were synthesized, especially at 220 and 234 amu. |
| Phthalic | 2.1-6.25 | Much of the molecule survives at 4 km $sec^{-1}$ and decreases in abundance at higher impact velocities (up to 6.25). |
| Nogoya | 4.3-6.1 | Carbonaceous chondrite that contains more water, bulk C, and somewhat different organic chemistry than Murchison. PAHs between mass 178 and 206 amu partially survived impact, although those above 240 amu were also destroyed. Additional alkyl homologs of phenanthrene/anthracene were synthesized, especially at 220 and 234 amu. |

## ACKNOWLEDGEMENTS

We thank the LDEF Project Office and the NASA Exobiology Program for support of this work.

## REFERENCES


1. Bunch, T. E.; Becker, L.; Bada, J.; Macklin, J.; Radicati di Brozolo, F.; Fleming, R. H.; and Erlichman, J.: Hypervelocity impact survivability experiments for carbonaceous impactors. *Second LDEF Sym. NASA* **CP-3194**, 453-477, 1993.

2. See, T.; Allbrooks, M.; Atkinson, D.; Simon, C.; and Zolensky, M.: Meteoroid and debris impact features documented on the Long Duration Exposure Facility a preliminary report. *Planet. Sci Branch Publ.* **# 84** (JSC **# 24608**), 1990.

3. Hörz, F.; Bernhard, R. P.; Warren, J.; See, T.; Brownlee, D. E.; Laurance, M. R.; Messenger, S.; and Peterson, R. B.: Preliminary analysis of LDEF instrument A0187-1 "Chemistry of micrometeoroids experiment". *First LDEF Sym. NASA* **CP-3134,** 487-499, 1992.

4. Bunch, T. E.; Radicati di Brozolo, F.; Fleming, R. H.; Harris, D. W.; Brownlee, D. E.; and Reilly, T.: LDEF impact craters formed by carbon-rich impactors: A preliminary report. *First LDEF Sym. NASA* **CP-3134**, 549-564, 1992.

5. Peterson, E.; Hörz, F.; Haynes, G.; and See, T.: Modification of amino acids at shock pressures of 3 to 30 GPa. *Meteoritics* **26**, 384, 1991.

6. Lewis, R. S.; Tang, M.; Wacker, J. F.; Anders, E.; and Steel, E.: Interstellar diamonds in meteorites. *Nature* **326**, 160-162, 1987.

7. Allamandola, L. J.; Sandford, S. A.; Tielens, A. G. G. M.; and Herbst, T. M.: Diamonds in dense molecular clouds: A challenge to the standard interstellar paradigm. *Science* **260**, 64-66, 1993.

8. Allamandola, L. J.; Sandford, S. A.; and Wopenka, B.: Interstellar polycyclic aromatic hydrocarbons and carbon in interplanetary dust particles and meteorites. *Science* **237**, 56-59, 1987

9. Langevin, Y.; Kissel, J.; Bertaux, J-L.; and Chassefiére E.: First statistical analysis of 5000 mass spectra of cometary grains obtained by PUMA 1 (Vega 1) and PIA (Giotto) impact ionization mass spectrometers in the compressed modes. *Astron. Astrophys.* **187**, 761-766, 1987.

10. Hahn, J.H.; Zennobi, R.; Zare, R.N.: Subfemtomole quantitation of molecular absorbates by two-step laser mass spectrometry. *J. Amer. Chem. Soc.* **109**, 2842-2843, 1987.

11. Engelke, F.; Hahn, J.H.; Henke, W.; Zare, R.N.: Determination of phenythiohydrandion-amino acids by two-step laser desorption/multiphoton ionization. *Anal. Chem.* **59**, 909-912, 1991.

12. Hillenkamp, F.; Karas, M.; Beavis, R.C.; Chait, B.T.: Matrix-assisted laser desorption/ionization mass spectrometry of biopolymolecules. *Anal. Chem.* **63**, 24-37, 1991.

13. Zenobi, R.; et al.: Spatially resolved organic analysis of the Allende meteorite. *Science* **24**, 1026-1028, 1989.

14. *Handbook of Chemistry and Physics*, 67th edition. The Chemical Rubber Co., Cleveland, OH 1987.

15. Ishiwatari, R. and Fukushima, K.: Generation of saturated and aromatic hydrocarbons by thermal alteration of young kerogen. *Geochim. Cosmochim. Acta* **43,** 1343-1349, 1979.

16. Wing, M. R. and Bada, J. L.: Geochromatography on the parent body of the carbonaceous chondrite Ivuna. *Geochim. Cosmochim. Acta* **55**, 2937-2942, 1991.

17. Blumer, M.: Polycyclic aromatic compounds in nature. *Sci. Amer.* **234** no. 3, 34-38, 1976.

18. Vedder, J. F.: Microparticle accelerator of unique design. *Rev. of Sci. Instr.* **49**, 1-7, 1978.

19. Cintala, M. J.: Impact-induced thermal effects in the Lunar and Mercurian regolith. *J. Geophy. Res.* **97**, 947-973, 1993.

20. Bernhard, R. P.; See, T. H. and Hörz, F.: Projectile compositions and modal frequencies on the "Chemistry of micrometeoroids" LDEF experiment. *Second LDEF Sym.* **NASA CP-3194**, 551-573, 1993.

21. Hörz, F.; Fechtig, H. and Janicke, J: Morphology and chemistry of projectile residues in small experimental craters. *Proc. 14th LPSC, J. Geophy. Res.* **88**, B353-363, 1983.

22. Huss, G. R.: Ubiquitous interstellar diamond and SiC in primitive chondrites: Abundances reflect metamorphism. *Nature* **347**, 159-162, 1990.

23. Aihara, Jun-ichi: Why aromatic compounds are stable. *Sci. Amer.* **240**, no. 3, 62-68, 1992.